Wilkens, R.H., Firth, J., Bender, J., et al., 1993
Proceedings of the Ocean Drilling Program, Scientific Results, Vol. 136

4. PLIOCENE–PLEISTOCENE VOLCANIC SANDS FROM SITE 842: PRODUCTS OF GIANT LANDSLIDES[1]

Michael O. Garcia[2]

ABSTRACT

Several distinct, thin (2–7 cm), volcanic sand layers ("ashes") were recovered in the upper portions of Holes 842A and 842B. These holes were drilled 320 km west of the island of Hawaii on the outer side of the arch that surrounds the southern end of the Hawaiian chain. These layers are Pliocene to Pleistocene in age, graded, and contain fresh glass and mineral fragments (mainly olivine, plagioclase, and clinopyroxene) and tests of Pleistocene to Eocene radiolarians. The glass fragments are weakly vesicular and blocky to platy in shape. The glass and olivine fragments from individual layers have large ranges in composition (i.e, larger than expected for a single eruption). These features are inconsistent with an explosive eruption origin for the sands. The only other viable mechanism for transporting these sands hundreds of kilometers from their probable source, the Hawaiian Islands, is turbidity currents. These currents were probably related to several of the giant debris slides that were identified from Gloria sidescan images around the islands. These currents would have run over the ~500-m-high Hawaiian Arch on their way to Site 842. This indicates that the turbidity currents were at least 325 m thick.

Paleomagnetic and biostratigraphic data allow the ages of the sands to be constrained and, thus, related to particular Hawaiian debris flows. These correlations were checked by comparing the compositions of the glasses from the sands with those of glasses and rocks from islands with debris flows directed toward Site 842. Good correlations were found for the 110-ka slide from Mauna Loa and the ~1.4-Ma slide from Lanai. The correlation with Kauai is poor, probably because the data base for that volcano is small. The low to moderate sulfur content of the sand glasses indicates that they were derived from moderately to strongly degassed lavas (shallow marine or subaerially erupted), which correlates well with the location of the landslide scars on the flanks of the Hawaiian volcanoes. The glass sands may have been formed by brecciation during the landslide events or spallation and granulation as lava erupted into shallow water.

INTRODUCTION

One of the main objectives for drilling at Site 842 was to evaluate the contribution of Hawaiian explosive volcanism to the deep-sea sediments downwind from the main Hawaiian Islands. This was being evaluated because several previous studies (Edsall, 1975; Rehm and Halbach, 1982) have proposed that ashes from the Hawaiian Islands have made a significant contribution to the sediments around the islands. Site 842 is located southeast of the Hawaiian Islands on the arch that surrounds the southern end of the Hawaiian chain (Fig. 1). The arch rises about 500 m above the Hawaiian Deep; thus, it was assumed that the only products from Hawaiian volcanoes to reach the drill site would be airborne ash.

Ash is not generally considered a common product of Hawaiian shield volcanoes. Typical Hawaiian eruptions are effusive with low lava fountains (<50 m) that produce little ash (Walker, 1990). However, there are two historic examples of violent explosions from Kilauea Volcano on the island of Hawaii. The explosions produced ash clouds that probably rose many tens of kilometers above the vent. The most violent event occurred in 1790, when a base surge killed more than 60 people and deposited up to 12 m of ash at the crater rim (McPhie et al., 1990). The other eruption occurred in 1924 and was phreatic but produced little ash (Decker and Christiansen, 1984). Several prehistoric ash horizons on Kilauea are 0.5 to 16 m thick (Decker and Christiansen, 1984). The composition of the magma erupted during this stage is tholeiitic (e.g., Wright, 1971).

Ash is also generated from Hawaiian volcanoes during their post-shield stage. For example, Mauna Kea Volcano has widespread deposits of silt-size, hawaiitic composition ash up to 2 m thick on its downwind side (Porter, 1979). However, effusive products greatly dominate the volume of volcanic material produced during this stage, and the magma supply rate is 15 to 60 times less than during the shield stage (Moore et al., 1987). The post-erosional stage of volcanism in Hawaii has generated extremely violent eruptions, but produced only small volumes of basanitoid to nephelinitic ash (~0.00001 km^3/year; Walker, 1990).

The greatest amount of airborne ash from Hawaiian shield volcanoes probably occurs when they emerge above sea level. During this stage, copious quantities of ash can be produced (perhaps 0.1 km^3/year based on the average magma supply for Hawaiian shield volcanoes; e.g., Dzurisin et al., 1984) as magma and seawater react violently (see Kolelaar [1986] for a discussion of this process). A small-scale example of this type of eruption is the 1963–64 eruption of Surtsey, south of Iceland (Thorarinsson, 1967).

Before Leg 136, it was envisioned that ash produced during surtseyan-type eruptions might be transported downwind a considerable distance by the strong northeast trade winds (25 to 50 km/hr with gusts to 65 km/hr) that blow over the Hawaiian Islands. The ash produced during these eruptions would be characterized by high vesicularity (40 to 50 vol%; Moore, 1985) and limited variation in composition within individual ash horizons (e.g., Batiza et al., 1984).

Several distinct, "ash-rich" layers (1 to 2 cm thick) were recovered during drilling on Leg 136 in the upper portions of Holes 842A and 842B. These holes, which are 10 m apart, were drilled 320 km west of the Island of Hawaii on the arch that surrounds the southern end of the chain. These layers are normally graded and contain fresh glass and mineral fragments (mainly olivine, plagioclase, and clinopyroxene) and tests of Quaternary and Eocene radiolarians. The glass fragments are weakly vesicular and have a large range in composition within individual layers. The olivine in these layers has a large and heterogeneous compositional range. These features indicate mixing during transport and deposition and are inconsistent with an airborne ash origin. Giant landslides are known to have occurred periodically on the flanks of the Hawaiian Islands (e.g, Moore et al., 1989). These giant landslides produced debris flows that may have deeply eroded

[1] Wilkens, R.H., Firth, J., Bender, J., et al., 1993. *Proc. ODP, Sci. Results,* 136: College Station, TX (Ocean Drilling Program).

[2] Hawaii Center for Volcanology, Geology and Geophysics Department, University of Hawaii, Honolulu, HI 96822, U.S.A.

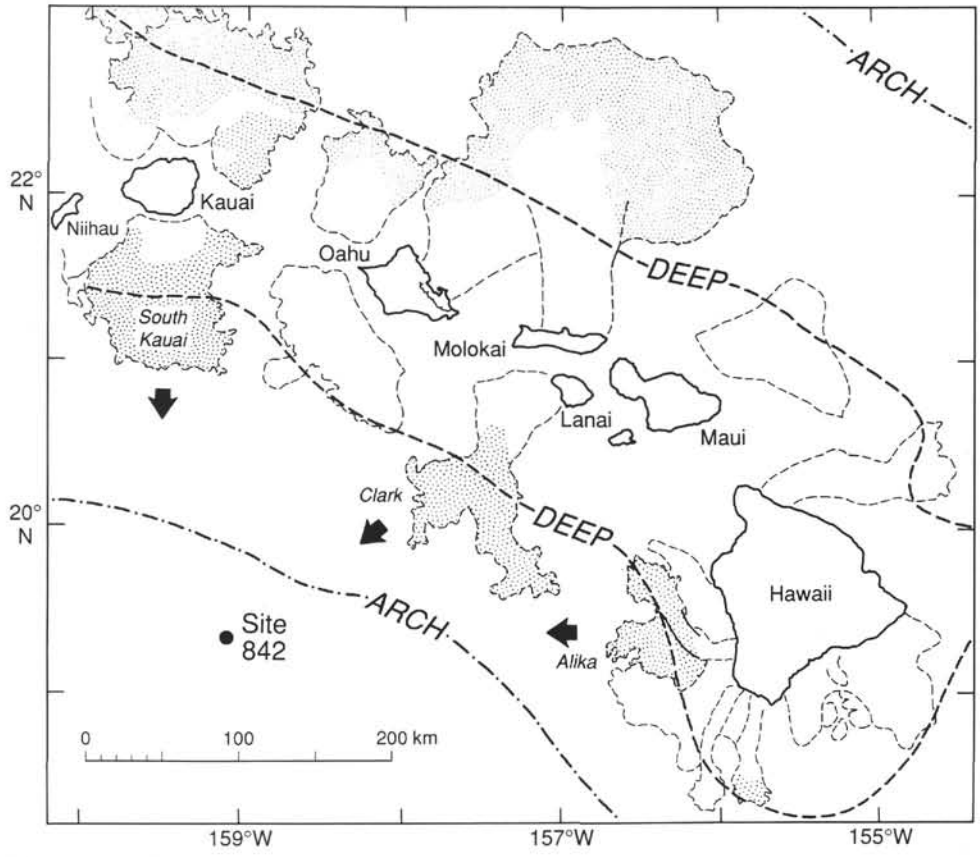

Figure 1. Map of the Hawaiian Islands showing major landslides (bounded by light dashed lines). The debris flows associated with these slides are shown by the stippled pattern. The debris flows that traveled toward Site 842 are the Alika Slide from Mauna Loa Volcano, Clark Slide from Lanai Volcano, and the South Kauai Slide from Kauai (after Moore et al., 1989). The axis of the Hawaiian deep is shown by the heavy dashed line; the Hawaiian arch axis is shown by the heavy dashed-dotted line.

the soft sediment section around the islands. Although these debris flows stopped on the island-side of the Hawaiian Arch (Moore et al., 1989), they were probably accompanied by turbidity currents that transported these volcanic sands across the arch. On the basis of the experiments of Muck and Underwood (1990), the turbidity currents must have been >325 m thick to have crossed the Hawaiian Arch.

STRATIGRAPHY

Volcanic sand is common throughout the 9.5 m of core recovered from Hole 842A and the upper 14 m of core from Hole 842B (Fig. 2). It occurs as disseminated grains with pelagic sediment and in discrete layers. The base of these layers is sharp; the glass grain size fines upward and grades into the overlying brown clay. Hole 842A has four distinct sand-rich layers; Hole 842B has three in the lower part of Core 2H (Fig. 2). The cores contain many remnants of sand-rich horizons that are now disrupted into round to elongate globules 2-4 mm wide. These sections of the core were probably disrupted by bioturbation. Much of the rest of both cores contains finely disseminated volcanic glass that gives the core a light brown to dark grayish-brown color. However, there are zones 5 to 65 cm thick in both holes that are tan and contain little or no volcanic glass (see Fig. 2).

The age of the volcanic sand layers can be constrained by paleomagnetic data (using the new time scale of McDougall et al., 1992) and biostratigraphy. The youngest layer from the upper part of Hole 842A (~25 cm below seafloor) is from a normally polarized, 200-cm-thick section of sediment (Fig. 2). It may be ~100 ±20 ka, assuming a constant sedimentation rate at the site and no erosion associated with deposition of the sand. This age is consistent with the absence of the radiolarian species *Axoprunum angelium* in a sample taken 3 cm below the sand layer. This species last occurred about 0.36 +0.02 Ma (Hull, this volume). A zone of bioturbated sand from Core 842A-1H-2 at 138 cm is from near the middle of a reversely magnetized section (Shipboard Scientific Party, 1992) that was probably deposited between 0.78 and 0.99 Ma.

The lower three sand layers from Hole 842A are from near the bottom of a reversely magnetized section (Matuyama; 1.07 and 1.78 Ma; Shipboard Scientific Party, 1992). They are probably 1.4 to 1.6 Ma based on estimates of sedimentation rates from paleomagnetic data. This is consistent with the presence of nannofossils assignable to the lower part of Quaternary Zone NN19 in a sample taken between the bottom two sand layers in this hole (Hull, this volume). In particular, the presence of *Calcidiscus macintyrei,* whose last occurrence was at 1.3 Ma (Hull, this volume), in sediment between sand layers 3 and 4 (see Fig. 2) places a minimum age for these sands. These sand layers also contain an assemblage of poorly to moderately preserved, early to middle Eocene radiolarians (Hull, this volume). Eocene radiolarians are not present in sediment above or below the sand layers. Hull (this volume) interpreted the presence of both Quaternary and Eocene radiolarians in the sand layers to be caused by reworking.

There are three volcanic glass sand layers in Hole 842B, Core 2H at 13 to 14 mbsf. They are in a reversely magnetized section (Fig. 2) that was inferred to have been deposited during the early part of the Gauss magnetic interval (3.2 to 3.4 Ma; Shipboard Scientific Party, 1992). However, the location of the Gauss reversal event in this core

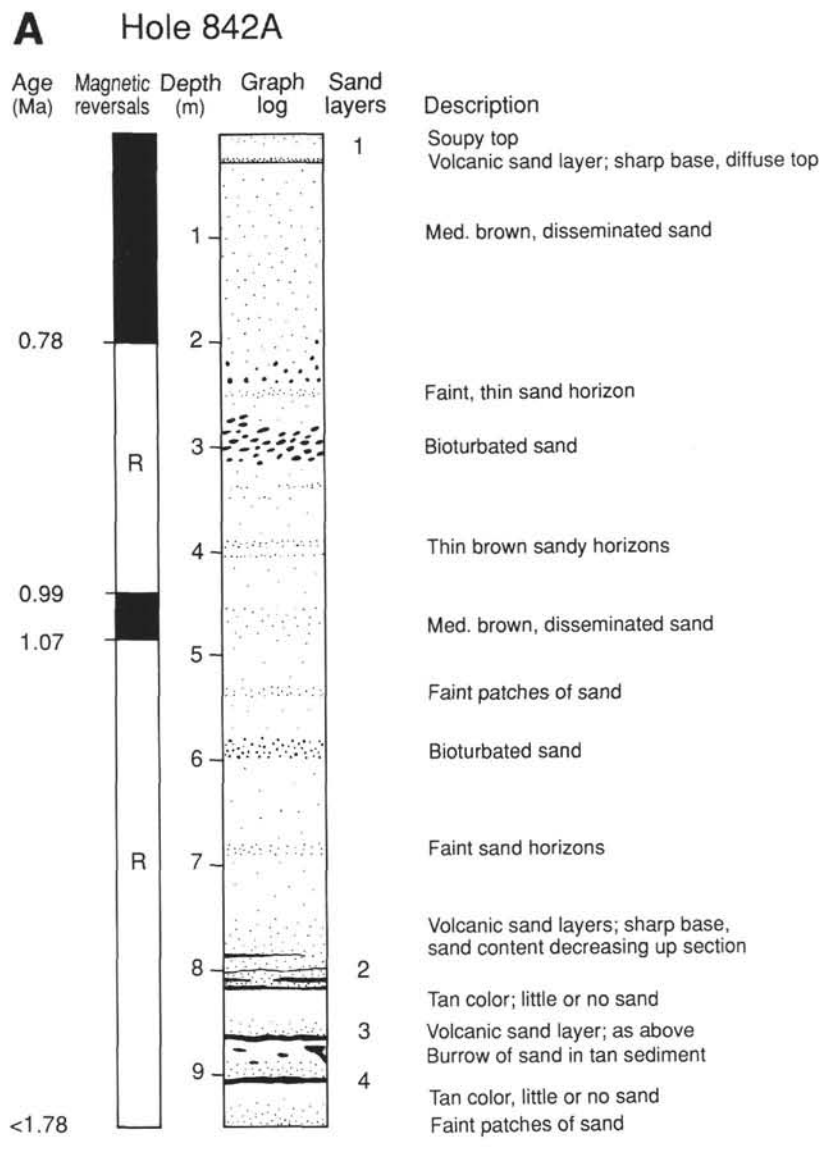

Figure 2. Summary logs of the sand distribution in and inferred magnetic polarity of Pliocene–Pleistocene sediments from **(A)** Hole 842A and **(B)** Cores 1H and 2H from Hole 842B. The magnetic polarity determinations are from Shipboard Scientific Party (1992); polarity ages are from McDougall et al. (1992).

is somewhat ambiguous because the top of Core 2H has a mixed magnetic signature. Re-examination of the core showed that this zone is "soupy" material. Apparently, it is common for the second advanced piston corer (APC) core from the same hole to recover slumped material (John Miller, pers. comm., 1992). However, if the drillers' depths in the hole are correct, and the two Reunion subchrons are recorded as one normal interval (there is only about a 4,000-year interval between them; McDougall et al., 1992), then the paleomagnetic age for these sands is 2.75 to 3.0 Ma. Unfortunately, Core 2H is barren for microfossils (Hull, this volume), so we have no independent method to verify this interpretation.

PETROGRAPHY

The volcanic sand layers are heterogeneous. Their main components are glass (50–80 vol%), clay (<1 to 20 vol%), biogenic material (radiolarian tests and sponge spicules; <1 to 5 vol%), olivine (<1 to 3 vol%), plagioclase (<1 to 3 vol%), and clinopyroxene (<1 vol%). Glass and mineral fragments range in size from 0.01 to 0.42 mm in length. All of the fragments are anhedral. Virtually all (>99%) of the glass fragments are blocky or platy (see Fig. 3). Some are strongly elongate (aspect ratios up to 1 to 8). Bubble-wall forms are uncommon (<5%). The glass fragments range in appearance from fresh to completely altered. The fresh glass is clear and tan to light brown. An equal proportion of the glass fragments are cloudy to opaque and dark gray in thin section. Altered glass is yellowish to reddish and, in the extreme cases, has completely altered to clay. Altered glass is rare (<1 vol%) in the upper part of the cores (<10 mbsf), but predominates in the deeper samples in Hole 842B.

The mineral fragments are fresh throughout the portion of the core examined here (upper 14 mbsf). Olivine fragments are generally larger and more abundant than plagioclase and clinopyroxene fragments.

GEOCHEMISTRY

Methods

The University of Hawaii electron microprobe was used to determine the composition of glass and olivine fragments. For the glasses,

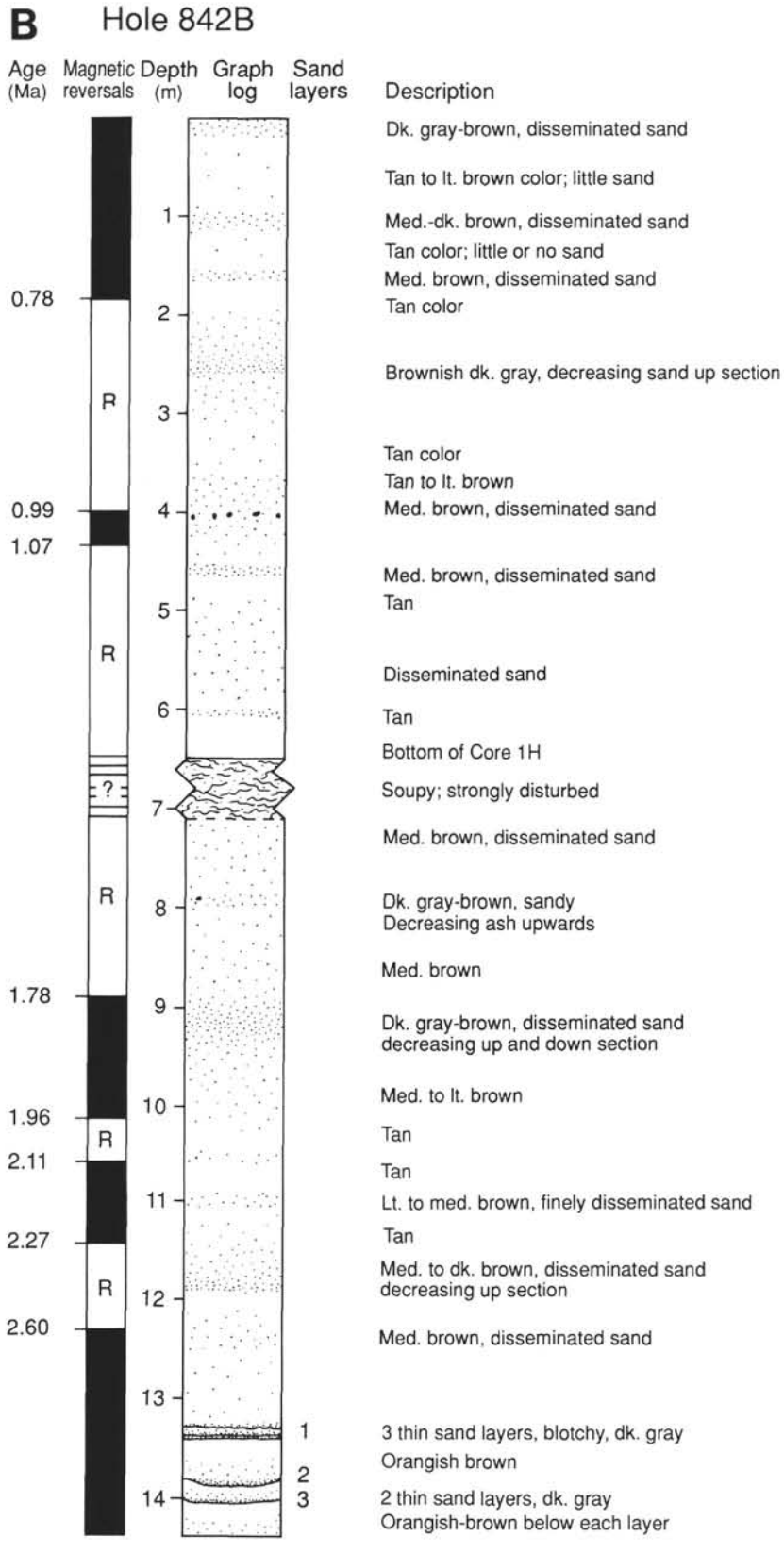

Figure 2 (continued).

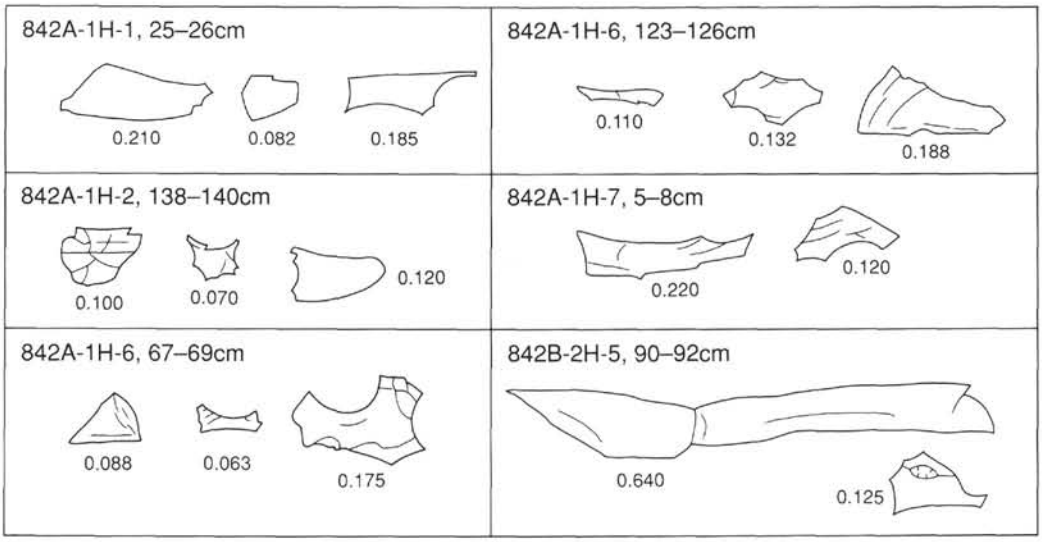

Figure 3. Shapes and sizes (in mm) of glass fragments from Site 842 as seen in thin section. Glass grains are blocky to platy in shape. Vesicles are uncommon in most glass fragments. The angular and elongate shape of many grains indicates that they experienced little abrasion during transport.

beam conditions were 15 kV with a 10-nA sample current and a 15-μm beam diameter. Peak counting times were 20 s for most elements, except Mn and P (50 s). Na was analyzed first in each analysis to minimize the possibility of its loss during analysis. The Smithsonian glass standards VG-2 and A99 were used for calibration and to monitor calibration drift. Precision for major elements (i.e., > 1 wt%) is 1% to 2% relative; for minor elements, it is 5% to 10% relative. For glass sulfur analyses, a troilite standard was employed; counting times of 200 to 400 s were used. Precision for S analyses is estimated to be 5% to 10% relative based on repeated analyses of a glass standard. For olivine, a focused beam at 15 kV with a sample current of 15 nA was used. Peak counting times were 30 s. Precision for olivine analyses is estimated to be <0.5% forsterite based on repeated analyses of an olivine standard. A ZAF correction scheme was employed to obtain the final analyses reported in Tables 1 and 2.

Glass

Analyses were made of at least 20 glass fragments per sample. All the different morphologies present within a sample were analyzed. The totals for most of the major element analyses are 99.5% +0.5% (Table 1), which indicates that the glasses are fresh and may contain relatively low volatile contents. A study of Hawaiian tholeiitic submarine glasses collected in water depths between 1 and 4 km showed that they contain total volatile contents between 0.3 and 0.9 wt% (Garcia et al., 1989).

To gain a better estimate of the volatile content of the Leg 136 volcanic glass sands, sulfur analyses were made on 5 to 7 grains per sample on both light brown and dark gray glasses using the electron microprobe. All of these glasses have low S contents (<0.06 wt%, most <0.02 wt%; see Fig. 4), and there is no systematic S content difference between the light and dark glasses. Typical Hawaiian submarine tholeiitic glasses have S contents >0.04 wt%; subaerially erupted tholeiitic glasses have S contents <0.015 wt% (see Fig. 4). Thus, the Leg 136 volcanic sand glasses were probably erupted under shallow marine to subaerial conditions that allowed partial degassing of the lava before solidification.

The glasses from volcanic sand-rich layers are all tholeiitic (Fig. 5) and similar in composition to Hawaiian tholeiites as opposed to other types of tholeiites (e.g., >0.30 wt% K_2O; see Table 1). The compositional variation among the Site 842 glasses spans the entire range of the current data base for Hawaiian tholeiitic glasses (excluding the

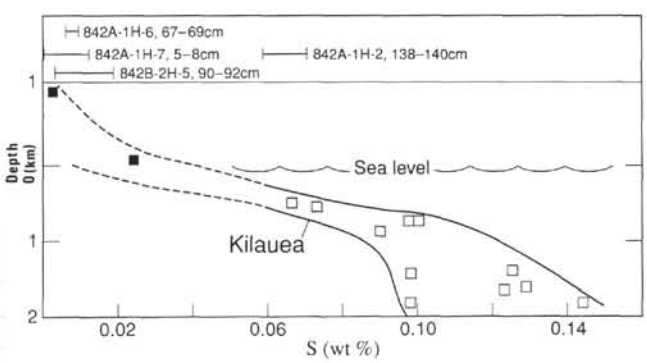

Figure 4. Sulfur content of some Site 842 glasses. The brackets show the range of sulfur contents for 8 to 10 glass fragments per sample. The variation of S content in Kilauea volcanic glasses vs. depth (above and below sea level) is shown for comparison. The low S content of most of the Site 842 glasses indicates they were at least partially degassed at the time of quenching. Solid boxes are for subaerially erupted samples; open boxes are for submarine erupted samples. Data for Kilauea samples from Byers et al. (1985), Dixon et al. (1991), and D. Muenow (unpubl. data).

preshield tholeiites from Loihi). This reflects, in part, the limited number of glass analyses for older Hawaiian volcanoes. However, the compositional variability of the Site 842 glasses may also indicate that the sands are sampling a larger portion of Hawaiian volcanoes than has been sampled subaerially or from dredging the submarine flanks.

Within individual layers, there are wide ranges in TiO_2 at a given MgO content (Fig. 6). These wide ranges are well beyond those that could be caused by crystal fractionation of the observed minerals (olivine, clinopyroxene, and plagioclase). This is especially true for the more mafic glasses (>7.0 wt% MgO; so-called olivine-controlled Hawaiian lavas; Wright, 1971). Olivine fractionation could not cause such wide variations in TiO_2 at a given MgO content. For comparison, the field for lavas from the current long-lived (10+ yr), Puu Oo eruption of Kilauea Volcano is relatively narrow despite the complex history of crystal fractionation of olivine, clinopyroxene, and plagioclase and magma mixing that these lavas have experienced (Garcia et al., 1992). Thus, the wide range in sand glass compositions within individual sand layers must reflect lavas that were derived from many different parental

Table 1. Representative microprobe major element analyses (in wt%) of glass fragments from Site 842.

SiO_2	TiO_2	Al_2O_3	FeO	MnO	MgO	CaO	Na_2O	K_2O	P_2O_5	Sum
842A-1H-1, 25–26 cm										
51.00	1.87	12.30	10.42	0.17	11.74	9.14	2.07	0.31	0.16	99.18
50.77	2.29	12.82	10.70	0.17	9.46	10.38	2.41	0.45	0.25	99.70
52.77	1.77	14.22	9.62	0.22	7.98	10.96	2.27	0.28	0.16	100.25
51.40	2.69	14.08	10.64	0.17	7.91	10.39	2.53	0.49	0.26	100.56
51.65	2.28	14.00	9.65	0.17	7.72	10.79	2.25	0.38	0.19	99.08
51.75	1.97	14.47	9.68	0.19	7.65	11.29	2.27	0.29	0.13	99.69
51.99	2.12	13.96	9.66	0.20	7.63	11.53	2.24	0.30	0.16	99.79
51.82	1.98	14.08	10.23	0.18	7.53	11.42	2.25	0.27	0.13	99.89
53.74	1.83	13.94	9.40	0.16	7.43	10.50	2.36	0.25	0.12	99.73
52.22	2.03	13.84	10.38	0.17	7.37	10.98	2.24	0.33	0.16	99.72
51.95	2.32	13.99	10.12	0.18	7.23	11.14	2.25	0.34	0.19	99.71
53.35	1.91	14.47	9.18	0.15	7.22	10.77	2.24	0.30	0.20	99.79
53.30	2.00	14.30	9.44	0.15	7.21	10.81	2.22	0.29	0.16	99.88
53.09	2.11	13.79	10.10	0.19	7.16	10.88	2.29	0.33	0.14	100.08
51.51	2.02	14.52	10.03	0.14	7.11	11.30	2.22	0.27	0.17	99.29
51.95	2.12	14.27	9.88	0.16	7.08	11.51	2.20	0.33	0.15	99.65
52.27	2.08	13.80	10.64	0.19	7.04	11.02	2.17	0.29	0.14	99.64
52.85	2.10	14.15	9.90	0.15	7.01	10.93	2.26	0.31	0.13	99.79
52.34	2.18	14.31	9.85	0.18	6.95	11.01	2.23	0.34	0.19	99.58
51.28	2.50	14.21	10.02	0.17	6.94	11.62	2.31	0.41	0.20	99.66
52.15	2.38	14.05	9.95	0.20	6.93	11.27	2.22	0.36	0.19	99.70
51.95	2.60	14.35	9.39	0.17	6.92	11.09	2.42	0.39	0.17	99.45
51.15	2.34	13.92	10.50	0.18	6.91	11.42	2.25	0.37	0.19	99.23
52.30	2.20	14.65	9.89	0.16	6.91	11.00	2.29	0.35	0.18	99.93
51.40	2.59	13.90	10.33	0.13	6.88	11.64	2.23	0.40	0.17	99.67
51.20	2.30	14.18	10.41	0.19	6.87	11.46	2.26	0.35	0.18	99.40
52.05	2.22	14.11	10.00	0.17	6.80	11.23	2.25	0.34	0.21	99.38
52.82	2.11	13.83	10.61	0.24	6.67	11.00	2.35	0.39	0.20	100.22
51.70	2.36	14.10	10.07	0.21	6.53	11.19	2.32	0.38	0.20	99.06
842A-1H-2, 138–140 cm										
51.05	2.33	13.10	11.20	0.15	9.08	10.32	1.96	0.37	0.15	99.71
50.30	2.46	12.83	11.21	0.22	9.04	10.31	2.06	0.40	0.20	99.03
51.06	2.50	13.31	10.73	0.20	8.20	10.27	2.19	0.37	0.18	99.01
51.05	2.35	13.26	10.98	0.18	8.11	10.72	2.14	0.39	0.18	99.36
51.13	2.48	13.34	10.62	0.21	8.04	11.03	2.24	0.40	0.21	99.70
50.99	2.35	13.47	11.08	0.20	8.00	10.74	2.17	0.38	0.22	99.60
51.11	2.46	13.32	10.36	0.19	7.99	10.90	2.11	0.41	0.21	99.06
50.95	2.36	13.57	10.60	0.17	7.91	10.92	2.19	0.36	0.19	99.22
50.94	2.49	13.54	10.72	0.15	7.78	10.76	2.21	0.40	0.27	99.26
51.15	2.37	13.58	10.78	0.15	7.70	11.05	2.18	0.37	0.27	99.60
51.01	2.49	13.46	11.39	0.15	7.69	10.67	2.20	0.44	0.22	99.72
51.43	2.63	13.70	10.54	0.15	7.10	11.26	2.21	0.36	0.19	99.57
51.47	2.49	13.68	10.78	0.19	6.96	10.79	2.27	0.38	0.20	99.21
842A-1H-6, 67–69 cm										
51.71	2.10	13.65	10.98	0.14	8.15	10.42	2.20	0.26	0.16	99.77
53.07	2.44	13.51	10.06	0.14	8.08	10.50	1.76	0.16	0.18	99.90
51.72	2.24	13.81	10.78	0.18	7.09	10.85	2.18	0.25	0.18	99.28
52.41	2.01	13.95	10.48	0.16	7.08	10.67	2.20	0.25	0.16	99.37
52.32	2.37	14.40	10.38	0.22	6.95	10.61	2.42	0.39	0.21	100.26
52.86	2.06	14.43	9.92	0.17	6.81	10.30	2.36	0.31	0.19	99.41
52.44	2.15	14.09	9.77	0.18	6.71	10.99	2.21	0.34	0.22	99.10
52.07	2.22	14.30	10.23	0.16	6.65	10.57	2.45	0.37	0.19	99.20
53.01	2.15	13.90	10.80	0.17	6.55	10.90	2.20	0.31	0.14	100.13
53.79	1.97	14.09	9.44	0.17	6.53	10.22	2.43	0.33	0.23	99.20
52.72	2.65	13.74	10.46	0.17	6.52	10.54	2.34	0.34	0.18	99.66
52.95	2.44	14.11	10.54	0.15	6.41	10.66	2.35	0.43	0.19	100.23
52.39	2.51	13.82	11.07	0.20	6.39	10.86	2.39	0.35	0.22	100.20
842A-1H-6, 123–126 cm										
54.22	1.63	13.81	10.34	0.17	7.62	9.49	2.43	0.25	0.18	100.14
52.77	1.93	13.82	10.45	0.18	7.55	10.08	2.40	0.35	0.24	99.77
53.57	1.99	14.01	9.73	0.15	7.24	10.35	2.28	0.30	0.20	99.82
52.76	2.05	13.96	10.17	0.15	7.06	10.50	2.40	0.35	0.20	99.60
52.13	2.46	13.71	10.76	0.17	7.06	11.17	2.08	0.34	0.25	100.13
53.80	1.79	14.05	10.25	0.17	7.05	10.22	2.39	0.32	0.18	100.22
52.05	2.14	13.93	10.95	0.14	6.89	10.52	2.28	0.34	0.22	99.46
52.25	1.98	14.00	10.40	0.16	6.85	10.70	2.36	0.36	0.23	99.29
53.34	2.04	13.70	9.74	0.13	6.50	10.44	2.41	0.41	0.29	99.00
52.63	2.45	13.50	10.67	0.15	6.38	10.27	2.39	0.44	0.24	99.12
842A-1H-7, 5–8 cm										
52.62	2.29	14.22	9.97	0.18	7.85	10.65	2.18	0.32	0.16	100.44
52.15	2.33	13.85	10.42	0.18	7.67	10.57	2.19	0.32	0.21	99.89
53.35	2.20	14.07	9.33	0.16	7.43	10.33	2.40	0.36	0.21	99.84
52.02	2.42	14.28	10.04	0.17	7.05	10.46	2.44	0.38	0.23	99.49
53.12	2.48	13.87	9.80	0.16	7.02	10.33	2.29	0.49	0.23	99.79
54.54	1.70	14.65	8.85	0.19	7.00	9.39	2.78	0.24	0.18	99.52
52.10	2.40	14.30	10.14	0.16	6.88	10.82	2.33	0.31	0.17	99.61
50.97	2.57	14.17	10.53	0.17	6.77	10.85	2.44	0.45	0.18	99.10
53.29	2.21	14.18	9.53	0.21	6.73	10.56	2.40	0.35	0.20	99.66
52.66	2.26	14.51	9.79	0.20	6.65	10.62	2.46	0.37	0.22	99.74
53.10	2.53	14.17	9.62	0.17	6.53	10.48	2.41	0.48	0.21	99.70
52.38	2.52	13.51	11.12	0.19	6.40	10.60	2.23	0.28	0.19	99.42
54.87	1.84	14.33	8.60	0.14	6.36	9.49	2.73	0.40	0.23	98.99

Table 1 (continued).

SiO_2	TiO_2	Al_2O_3	FeO	MnO	MgO	CaO	Na_2O	K_2O	P_2O_5	Sum
842B-2H-5, 90–92 cm										
50.59	2.20	13.30	10.97	0.19	9.26	10.55	2.20	0.40	0.19	99.85
50.50	2.13	13.44	10.98	0.19	9.00	10.25	2.18	0.42	0.20	99.29
51.40	2.28	13.85	10.62	0.20	7.86	10.97	2.22	0.37	0.21	99.98
51.75	2.33	13.95	10.20	0.18	7.73	10.74	2.32	0.38	0.24	99.82
51.33	2.27	13.75	10.38	0.23	7.73	10.92	2.27	0.41	0.21	99.50
51.55	2.39	14.07	10.19	0.19	7.70	10.66	2.32	0.41	0.19	99.67
51.37	2.17	14.38	9.86	0.16	7.61	11.27	2.31	0.49	0.18	99.80
52.27	2.23	14.39	9.89	0.18	7.39	10.87	2.49	0.35	0.23	100.29
51.34	2.49	14.20	10.09	0.18	7.30	10.88	2.34	0.50	0.33	99.65
50.60	2.67	14.27	9.92	0.20	7.10	11.34	2.36	0.48	0.23	99.17
51.87	2.32	14.31	9.83	0.16	7.06	11.11	2.38	0.42	0.22	99.68
52.56	2.51	14.11	10.14	0.17	7.05	10.32	2.43	0.48	0.19	99.96
52.36	2.50	14.18	10.26	0.21	7.04	10.46	2.48	0.45	0.25	100.19
50.97	2.57	14.17	10.53	0.17	6.77	10.85	2.44	0.45	0.18	99.10
53.29	2.21	14.18	9.53	0.21	6.73	10.56	2.40	0.35	0.20	99.66
52.66	2.26	14.51	9.79	0.20	6.65	10.62	2.46	0.37	0.22	99.74

Table 2. Representative microprobe analyses of olivine grains from two sand layers, Site 842.

	Sample 842A-1H-6, 67–69 cm						Sample 842B-2H-5, 90–92 cm							Standards[a]			
														San Carlos		Springwater	
	A	B	C	D	E	F	A	B	C	D	E	F	G	Given		Given	
SiO_2	40.2	40.13	39.56	39.23	39.13	38.62	40.57	40.69	40.05	39.65	39.5	39.05	38.72	40.81	40.65	38.95	39.43
FeO	11.06	11.87	14.19	15.68	16.33	19.82	8.93	9.65	12.05	14.25	15.75	17.42	19.03	9.55	9.68	16.62	16.61
MnO	0.14	0.18	0.16	0.2	0.19	0.32	0.14	0.1	0.14	0.17	0.2	0.28	0.27	0.14	0.14	0.3	0.28
MgO	47.63	47.01	45.13	43.69	43.25	39.83	49.55	48.52	47.3	45.2	43.9	42.47	41.15	49.42	49.44	43.58	43.89
CaO	0.28	0.26	0.29	0.31	0.27	0.32	0.2	0.23	0.23	0.24	0.32	0.25	0.28	<0.05	0.1	0	0.01
Total	99.31	99.45	99.33	99.11	99.17	98.91	99.39	99.19	99.77	99.51	99.67	99.47	99.45	99.92	100.01	99.45	100.22
Fo%	88.5	87.6	85	83.2	82.5	78.2	90.8	90	87.5	85	83.2	81.3	79.4				

[a] As an indication of the accuracy of these analyses, the given (Jarosewich et al., 1979) and determined values are listed for two Smithsonian olivine standards.

magmas. On the basis of the relative homogeneity of historic and prehistoric Mauna Loa lavas (Rhodes, 1983), many thousands of years would be required to produce this variation for an individual volcano.

Olivine

The olivine fragments in the volcanic sands have a large and heterogeneous range in composition (Fig. 7). The range for individual layers is as large as that observed for olivine in the large suite of submarine basalts from the east rift zone of Kilauea Volcano (e.g., Sample 842B-2H-5, 90–92 cm; forsterite 90.8% to 79.4% vs. 90.3% to 77.8%; Clague et al., in press). However, the range for the layers is similar in magnitude to that observed for the long-lived, current eruption (1983 to present) of Kilauea (forsterite 88% to 73%; Garcia et al., 1992). Thus, olivine composition is apparently not a useful discriminant for evaluating the time period represented by individual sand layers, because Hawaiian shield lavas display a relatively restricted range in major element composition, and single eruptive events can produce as much compositional variation in olivine as observed on a regional scale.

Multiple analyses were made on the larger grains to determine if they are compositionally zoned. All are homogeneous (i.e., forsterite content varies by less than 1%). However, the original rims on these grains, where compositional zoning is most likely to have been present, were probably removed during transport.

DISCUSSION

Origin of the Volcanic Sand Layers

The Pliocene–Pleistocene sand layers from Site 842 have sharp basal contacts, graded bedding and Eocene radiolarians (Hull, this volume). The glasses within the layers are heterogeneous in composition, platy to blocky in shape, and have low vesicularity. These features are inconsistent with a pyroclastic origin and are better explained by a turbidity flow origin.

What was the source for the turbidity flows? There are many Cretaceous seamounts near Site 842 (see Shipboard Scientific Party, 1992). However, the fresh nature of most of the glass fragments and the similarity of the glass compositions to Hawaiian lavas (Figs. 5 and 8) indicate that the source of the sands was the Hawaiian Islands. Thus, the turbidites traveled at least 240 km from the nearest island (Oahu) and up and over the Hawaiian Arch, which has about 500 m of relief (see Fig. 1).

What was the nature of the turbidity flows? The presence of reworked Eocene radiolarians in the sand layers (Hull, this volume) indicates that the turbidites may be related to major erosional events. Recently, it has been recognized that giant landslides have formed on the submarine flanks of many Hawaiian volcanoes (Moore et al., 1989). These landslides provided the energy to drive debris flows that could have substantially eroded the unconsolidated deep-sea sediments. They have also occurred infrequently, as have the sand layers with the Site 842 cores.

The minimum height of the turbidity flows that deposited the sand layers at Site 842 can be estimated using the maximum run-up elevation that the flow encountered (Muck and Underwood, 1990). This height is approximately 500 m for the Hawaiian Arch near Site 842. Because the height of the turbidity flow must be at least 65% of the bathymetric obstruction to be able to crest the feature (Muck and Underwood, 1990), the turbidity flows that deposited the sand layers at Site 842 must have been at least 325 m thick. Similar-sized or larger turbidity flows have been interpreted to have formed from landslides off the northeastern flank of South America (Dolan et al.,

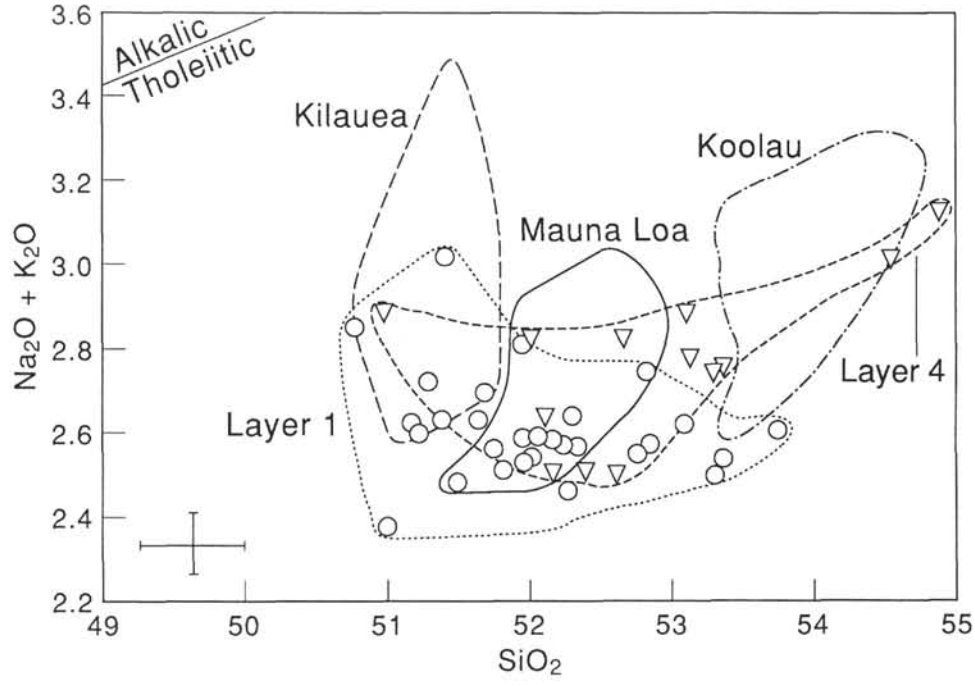

Figure 5. SiO_2 vs. total alkalis ($Na_2O + K_2O$) diagram for glasses from two Site 842 sand layers and several Hawaiian shield volcanoes. Note the large range in glass composition for the sand layers compared with glasses from some well-studied Hawaiian volcanoes. Fields for tholeiitic and alkalic lavas are from Macdonald and Katsura (1964). Data for Hawaiian glasses are from Garcia et al. (1989) for Kilauea and Mauna Loa, and Garcia (unpubl. data) for Koolau.

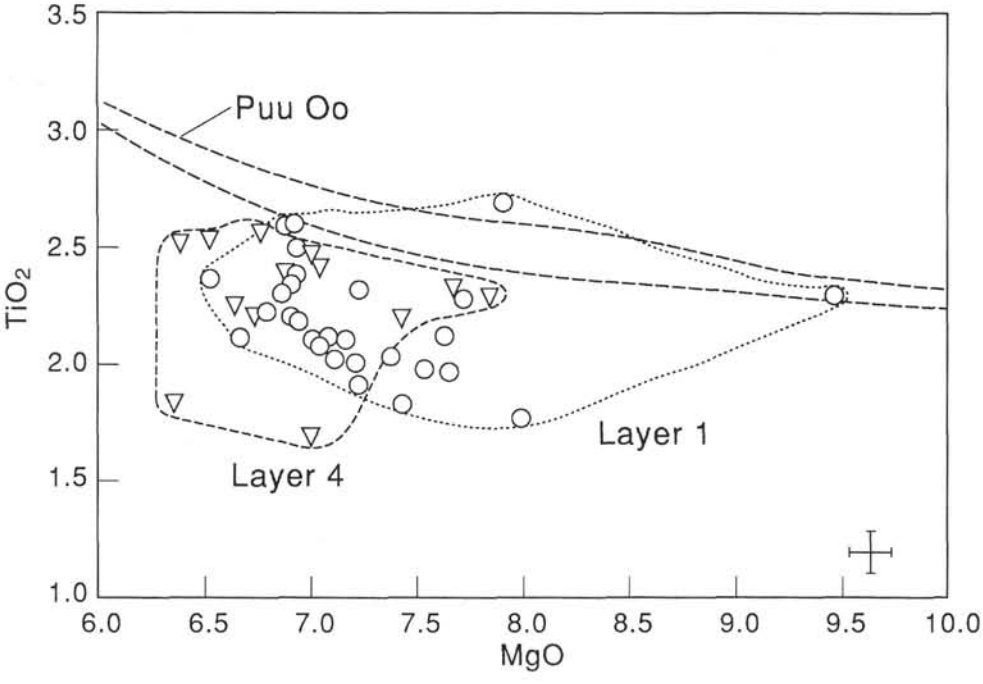

Figure 6. MgO vs. TiO_2 variation diagram for Site 842 glasses. The dashed field shows the lava compositions for the long-lived (9.5 yr) Puu Oo eruption of Kilauea Volcano (data from Garcia et al., 1992). The data for ODP samples are from Table 1. Note the wide range in TiO_2 content at a given MgO content for the Site 842 glasses compared with the Puu Oo lavas, which have experienced both magma mixing and crystal fractionation (Garcia et al., 1992).

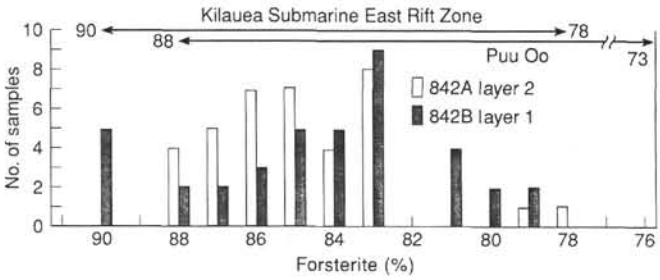

Figure 7. Histogram of olivine compositions (in % forsterite) in two sand layers from Site 842. For comparison, the olivine compositions for lavas from the long-lived Puu Oo eruption of Kilauea Volcano (Garcia et al., 1992) and pillow lavas from the submarine portion of Kilauea's east rift zone (Clague et al., 1993) are shown.

1989). A cartoon illustrating the turbidity flow model for the origin of the Site 842 sand layers is shown in Figure 9.

Correlation of Sand Layers with Specific Hawaiian Landslides

The age and petrology of the sand layers can be used to correlate the sands with specific Hawaiian landslides. Only three of these landslides formed debris flows that are directed toward Site 842. The youngest debris flow directed toward Site 842 is the Alika Slide from Mauna Loa. It has been dated at 105 ka (Moore et al., 1989). The next youngest debris flow pointed toward Site 842 is probably the Clark Slide from Lanai. The age of the slide is not known, but subaerial lavas from the island have been dated by K-Ar at about 1.2 to 1.5 Ma (Bonhommet et al., 1977), which serves as a maximum age for the Clark Slide. The other major slide directed toward Site 842 is from Kauai. The age of the South Kauai Slide is also unknown, but the age of shield building volcanism on the island has been dated at about 3.9 to 5.8 Ma (McDougall, 1979; Clague and Dalrymple, 1988).

The sand horizons in the cores that might correlate with these slides are 842A-1H-1, 25–27 cm, with Mauna Loa; 842A-1H-6, 63–69 cm, 842A-1H-6, 124–126 cm, and 842A-1H-7, 5–7 cm, with Lanai; and 842B-2H-5, 78–80 cm, 842B-2H-5, 90–91 cm, and 842B-2H-5, 136–138 cm, with Kauai. The paleomagnetic ages for the sand layers are consistent with these correlations (i.e., they are not older than the slides or volcanoes).

Comparison of glass compositions for the sand layers with glasses from these volcanoes is problematic for Lanai and Kauai, because no glass data have been published for either volcano (although a few unpublished glass analyses are available for Lanai). A visit was made to Kauai to collect glass from dike margins. Seventeen glassy dikes were sampled, but only 13 of these dikes have glass suitable for microprobe analysis. Seven of these glasses have MgO contents >6.4 wt% and all are less than 7.2 wt% (see Table 3). If glass compositions (and whole-rock compositions for Lanai and Kauai) are used, there is general agreement between the composition of the sand layers and that of the correlated volcano (Fig. 8) except for Kauai, which has a small data base. The correlations with Lanai and Kauai lavas need to be checked against pillow rim glasses from those volcanoes, because they may be different from the younger glasses that were sampled from the subaerial portions of those volcanoes.

Importance of Turbidity Currents to the Sediment Budget Around the Hawaiian Islands

Mixed radiolarian assemblages (typically Eocene and Quaternary) have been reported in cores taken from around the Hawaiian Islands (e.g., DSDP Sites 67 and 68; Winterer, Riedel, et al., 1971; Tracey, Sutton, et al., 1971). Early workers (e.g., Riedel and Funnel, 1964)

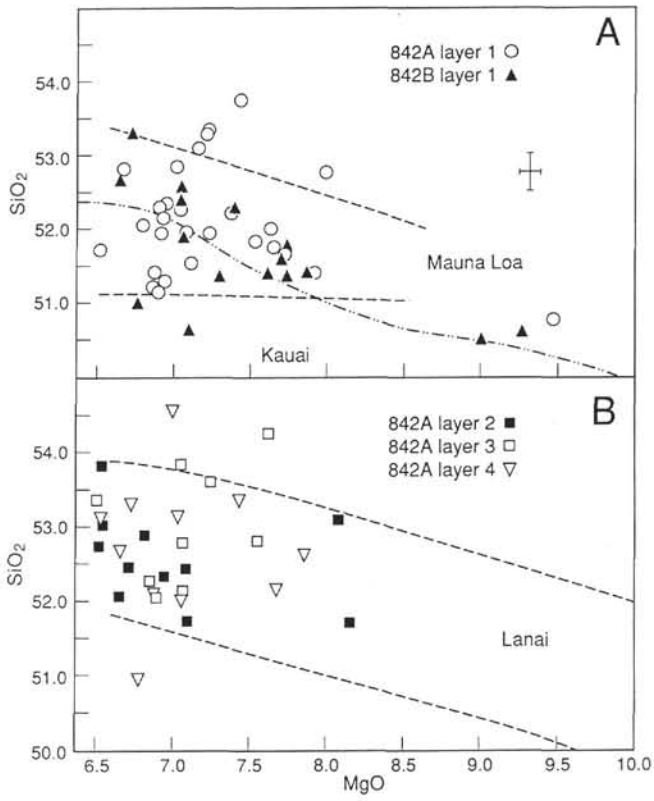

Figure 8. Comparison of SiO2 vs. MgO trends for glasses from individual sand layers with Hawaiian glasses (Mauna Loa and Lanai) and/or whole-rock (Lanai and Kauai) data (shown by dash lines). Data sources: Mauna Loa (Garcia et al., 1989; Moore and Clague, 1992); Lanai (Garcia, unpubl. data, for glass; West et al., 1992, for whole rock); Kauai (Macdonald and Katsura, 1964). **A.** Samples 842A-1H-1, 25–26 cm (Layer 1), 842B-2H-5, 90–92 cm (Layer 1), vs. Mauna Loa and Kauai, respectively. **B.** Samples 842A-1H-5, 67–69 cm (Layer 2), 842A-1H-6, 123–126 cm (Layer 3), and 842A-1H-7, 5–8 cm (Layer 4), vs. Lanai. Two sigma error bar shown for reference. The large range in glass composition for the sand layers may indicate that every layer sampled a larger range of samples than represented by our data base for these volcanoes.

attributed the mixed assemblages to bottom currents from Antarctica. However, one study noted that mixed assemblages were commonly associated with volcanic sand layers, which were interpreted as products of turbidity currents (Schreiber, 1969). These deposits were assumed to be of only local significance (i.e., within the Hawaiian Arch; Schreiber, 1969). However, similar deposits were found 930 km south of the Hawaiians in cores taken near the Clarion Fracture Zone (Rehm and Halbach, 1982). The volcanic glass sand layers in these cores are up to 30 cm thick, tholeiitic in composition, and 1 to 2 Ma in age, according to Rehm and Halbach (1982). They concluded that the sands originated from the island of Maui but could not have been deposited from turbidity currents because a 400-m-deep trough (which they felt formed long before the sand layers were deposited) is located 20 km north of the coring sites. They preferred an eolian origin for the sand layers despite the low to nonvesicular nature of the glass sand, and the up-to-30-cm thickness of the sandy layers. The Clarion site is southeast of the Hawaiian Islands, at a right angle to the prevailing northeasterly trade winds. Thus, it is unlikely that these volcanic sands are of pyroclastic origin. Instead, they may be products of turbidity currents associated with the catastrophic slope failures on the flanks of the Hawaiian Islands. If they are, some Hawaiian turbidity currents may travel vast distances (1,000+ km). Similar far-traveling turbidites have been reported near Barbados (Dolan et al., 1989).

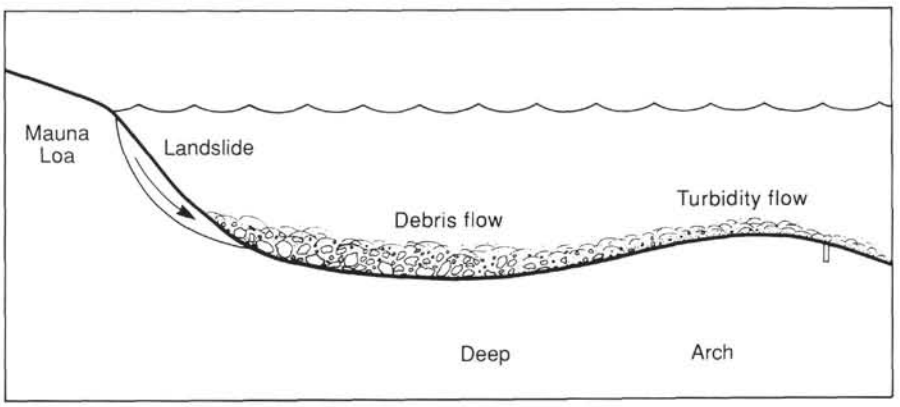

Figure 9. Cartoon illustrating the proposed relationship of landslides on the flanks of Hawaiian volcanoes to debris flows and turbidity flows that might have deposited sand layers at Site 842.

Formation of the Volcanic Sand

The relative scarcity of vesicles in the Site 842 glass grains precludes a pyroclastic cause for their origin (see Heiken and Wohletz, 1985). The platy to blocky shape and low vesicularity of the Site 842 glass grains are identical to glasses formed by hydroclastic eruptions (e.g., Fisher, 1968; Batiza et al., 1984). However, the sulfur content of the Site 842 glass sands is low, indicating they were erupted near or above sea level (e.g., Dixon et al., 1991). Large volumes of glass sand are produced during Hawaiian eruptions when lava enters the ocean for weeks to years as the volcano extends its coastline seaward (e.g., Moore et al., 1973). A preliminary examination of glasses formed as lava entered the ocean from the current Puu Oo eruption of Kilauea Volcano showed that they are moderately vesicular (K. Okano, pers. comm., 1993), unlike the Site 842 glasses. However, these glasses were collected from beaches, which may sample only the littoral component of this process. Granulation and thermal spallation in deeper water (e.g., Fisher, 1984), especially on the steep submarine slopes of Hawaiian volcanoes, may produce less vesicular glasses. Such hydroclasts have been reported from lavas that have undergone internal explosions (e.g., implosions; Fisher, 1984; Fisher and Smith, 1991). More work is needed to characterize the glass fragments produced during this process, because they may constitute a significant component of the sediments around Hawaiian volcanoes.

The landslide model for the origin of the Site 842 sand layers provides an additional mechanism for forming glass grains. During a landslide event, it is likely that glassy lavas are brecciated. The glassy margins of lava flows would have served as zones of weakness along which fragmentation could occur (see Fisher, 1984, for a more complete description of this process).

CONCLUSIONS

The Pliocene–Pleistocene sedimentary section at Site 842 contains abundant volcanic sand. This sand is present as disseminated grains within pelagic sediment and as distinct layers. The sand layers were probably deposited by turbidity currents derived from debris flows generated by landslides on the flanks of Hawaiian volcanoes. Paleomagnetic and glass composition data are consistent with the sources of these sand layers being Mauna Loa, Lanai, and Kauai volcanoes. The turbidity currents associated with these landslides may have traveled great distances (up to 1,000 km) and traveled over significant bathymetric highs and lows. Thus, they may have been enormous in size and energy.

ACKNOWLEDGMENTS

I gratefully acknowledge the help of Kaui Kim in the petrography and glass analyses of the sand layers and of Jennifer Parker with managing the glass composition data base and preparing figures for this report. Help from D. Hull and J. Resig on biostratigraphic questions was much appreciated. T. Wright and C. Schreiber assisted with reviewing the literature on Hawaiian turbidites. My thanks to T. Hulsebosch for maintaining the U.H. microprobe in superb working order and to K. Okano for access to her unpublished data on Puu Oo hydroclasts. The final figures were prepared by Brooks Bays and

Table 3. Microprobe analyses (in wt%) of Kauai dike margin glasses.

	SiO_2	TiO_2	Al_2O_3	FeO	MnO	MgO	CaO	Na_2O	K_2O	P_2O_5	Total
Waimea Canyon											
WC-2	51.65	3.26	12.40	11.68	0.18	7.02	11.20	2.10	0.57	0.36	100.42
WC-3	52.05	2.93	13.70	11.10	0.16	6.05	10.85	2.41	0.48	0.25	99.98
WC-4	51.15	2.77	13.51	11.18	0.17	6.53	10.99	2.18	0.44	0.31	99.23
WC-5	51.01	3.03	13.20	12.50	0.19	6.13	10.80	2.28	0.49	0.32	99.95
Niu Valley											
Niu-1b	52.25	2.97	14.02	10.95	0.17	6.44	11.40	1.68	0.62	0.26	100.76
Niu-2	51.70	2.28	14.10	10.48	0.17	6.93	11.42	2.25	0.35	0.20	99.88
Niu-3	51.95	2.72	13.27	11.65	0.17	6.22	10.79	2.42	0.48	0.20	99.87
North Shore											
Cave-2	51.90	2.75	13.45	11.56	0.17	6.20	10.46	2.34	0.43	0.32	99.58
Cave-3	52.25	2.28	13.86	10.53	0.16	6.74	10.84	2.36	0.32	0.26	99.60
Cave-4	52.27	2.26	13.85	10.55	0.16	6.62	10.85	2.34	0.31	0.25	99.46
Trail-5a	50.45	3.05	13.52	10.96	0.17	6.34	10.92	2.66	0.48	0.36	98.91
Trail-5b	50.95	2.80	15.45	9.90	0.15	5.65	11.42	2.83	0.41	0.32	99.88
Trail-6	50.95	3.24	13.40	11.70	0.17	6.04	10.60	2.60	0.51	0.36	99.57
Trail-7	51.55	2.24	14.12	10.35	0.16	7.12	11.50	2.15	0.33	0.18	99.70

Barbara Taylor. A review by R.V. Fisher of an early draft of this paper is gratefully acknowledged. This research was supported by NSF grant ODP-TAMRF 20505. This is SOEST contribution No. 3251.

REFERENCES*

Batiza, R., Fornari, D.J., Vanko, D.A., and Lonsdale, P., 1984. Craters, calderas, and hyaloclastites on young Pacific seamounts. *J. Geophys. Res.,* 89:8371–8390.

Bonhommet, N., Beeson, M.H., and Dalrymple, G.B., 1977. A contribution to the geochronology and petrology of the island of Lanai, Hawaii. *Geol. Soc. Am. Bull.,* 88:1282–1286.

Byers, C.D., Garcia, M.O., and Muenow, D.W., 1985. Volatiles in pillow rim glasses from Loihi and Kilauea volcanoes, Hawaii. *Geochim. Cosmochim. Acta,* 49:1887–1896.

Clague, D.A., and Dalrymple, G.B., 1988. Age and petrology of alkalic postshield and rejuvenated-stage lava from Kauai, Hawaii. *Contrib. Mineral Petrol.,* 99:202–218.

Clague, D.A., Moore, J.G., Dixon, J.E., and Friesen, W.B., in press. The mineral chemistry and petrogenesis of submarine lavas from Kilauea's east rift zone. *J. Petrol.*

Decker, R.W., and Christiansen, R.L., 1984. Explosive eruptions of Kilauea Volcano, Hawaii. *In Explosive Volcanism:* Washington, D.C. (National Academy Press), 122–132.

Dixon, J.E., Clague, D.A., and Stolper, E.M., 1991. Degassing history of water, sulfur, and carbon in submarine lavas from Kilauea volcano, Hawaii. *J. Geol.,* 99:371–394.

Dolan, J.F., Beck, C., and Ogawa, Y., 1989. Upslope deposition of extremely distal turbidites: an example from the Tiburon Rise, west-central Atlantic. *Geology,* 17:990–994.

Dzurisin, D., Koyanagi, R.Y., and English, T.T., 1984. Magma supply and storage at Kilauea volcano, Hawaii, 1956–1983. *J. Volcanol. Geotherm. Res.,* 21:177–206.

Edsall, D.G., 1975. Submarine geology of volcanic ash deposits: age, and magmatic composition of Hawaiian and Aleutian tephra; Eocene to Recent [Ph.D. dissert.]. Columbia Univ.

Fisher, R.V., 1968. Puu Hou littoral cones, Hawaii. *Geol. Rundsch.,* 57:837–864.

———, 1984. Submarine volcaniclastic rocks. *In* Kokelaar, B.P., and Howells, M.F. (Eds.), *Marginal Basin Geology: Volcanic and Associated Sedimentary Processes in Modern and Ancient Basins.* Geol. Soc. Spec. Publ. London, 16:5–28.

Fisher, R.V., and Smith, G.A., 1991. Volcanism, tectonics and sedimentation. *Spec. Publ.—Soc. Econ. Petrol. Mineral.,* 45:1–5.

Garcia, M.O., Muenow, D.W., Aggrey, K.E., and O'Neil, J.R., 1989. Major element, volatile, and stable isotope geochemistry of Hawaiian submarine tholeiitic glasses. *J. Geophys. Res.,* 94:10525–10538.

Garcia, M.O., Rhodes, J.M., Wolfe, E.W., Ulrich, G.E., and Ho, R.A., 1992. Petrology of lavas from Episodes 2–47 of the Puu Oo eruption of Kilauea volcano, Hawaii: evaluation of magmatic processes. *Bull. Volcanol.,* 55:1–12.

Heiken, G., and Wohletz, K., 1985. *Volcanic Ash:* Berkeley (Univ. of California Press).

Jarosewich, E., Parkes, A.S., and Wiggins, L.B., 1979. Microprobe analyses of four natural glasses and one mineral: an interlaboratory study of precision and accuracy. *Smithsonian Contrib. Earth Sci.,* 22:53–67.

Kolelaar, P., 1986. Magma-water interaction in subaqueous and emergent basaltic volcanism. *Bull. Volcanol.,* 48:275–289.

Macdonald, G.A., and Katsura, T., 1964. Chemical composition of Hawaiian lavas. *J. Petrol.,* 5:82–133.

McDougall, I., 1979. Age of shield-building volcanism of Kauai and linear migration of volcanism in the Hawaiian island chain. *Earth Planet. Sci. Lett.,* 46:31–42.

McDougall, I., Brown, F.H., Cerling, T.E., and Hillhouse, J.W., 1992. A reappraisal of the geomagnetic polarity time scale to 4 Ma using data from the Turkana Basin, East Africa. *Geophys. Res. Lett.,* 19:2349–2352.

McPhie, J., Walker, G.P.L., and Christiansen, R.L., 1990. Phreatomagmatic and phreatic fall and surge deposits from explosions at Kilauea volcano, 1790 A.D.: Keanakakoi ash member. *Bull. Volcanol.,* 52:334–354.

Moore, J.G., 1985. Structure and eruptive mechanisms at Surtsey volcano, Iceland. *Geol. Mag.,* 122:649–661.

Moore, J.G., and Clague, D.A., 1992. Volcano growth and evolution of the island of Hawaii. *Geol. Soc. Am. Bull.,* 104:1471–1484.

Moore, J.G., Clague, D.A., Holcomb, R.T., Lipman, P.W., Normark, W.R., Torresan, M.E., 1989. Prodigious submarine landslides on the Hawaiian Ridge. *J. Geophys. Res.,* 94:17465–17484.

Moore, J.G., Phillips, R.L., Grigg, R.W., Peterson, D.W., and Swanson, D.A., 1973. Flow of lava into the sea, 1969–1971, Kilauea volcano, Hawaii. *Geol. Soc. Am. Bull.,* 84:537–546.

Moore, R.B., Clague, D.A., Rubin, M., and Bohrson, W.A., 1987. Hualalai volcano: a preliminary summary of geologic, petrologic, and geophysical data. *Geol. Surv. Prof. Pap. U.S.,* 1350:571–585.

Muck, M., and Underwood, M., 1990. Upslope flow of turbidity currents: a comparison among field observations, theory, and laboratory models. *Geology,* 18:54–57.

Porter, S.C., 1979. Quaternary stratigraphy and chronology of Mauna Kea, Hawaii. *Geol. Soc. Am. Bull.,* 90:980–1093.

Rehm, E., and Halbach, P., 1982. Hawaiian-derived volcanic ash layers in equatorial northeastern Pacific sediments. *Mar. Geol.,* 50:25–40.

Rhodes, J.M., 1983. Homogeneity of lava flows: chemical data for historic Mauna Loan eruptions. *Proc. 13th Lunar Planet. Sci. Conf.* (Pt. 2). *J. Geophys. Res.,* 88 (Suppl.):A869–A879.

Riedel, W.R., and Funnell, B.M., 1964. Tertiary sediment cores and microfossils from the Pacific Ocean floor. *Q. J. Geol. Soc. London,* 120:305–368.

Schreiber, B.C., 1969. New evidence concerning the age of the Hawaiian Ridge. *Geol. Soc. Am Bull.,* 80:2601–2604.

Shipboard Scientific Party, 1992. Site 842. *In* Dziewonski, A., Wilkens, R., Firth, J., et al., *Proc. ODP, Init. Repts.,* 136: College Station, TX (Ocean Drilling Program), 37–63.

Thorarinsson, S., 1967. The Surtsey eruption and related scientific work. *Polar Rec.,* 13:571–78.

Tracey, J.I., Jr., Sutton, G.H., et al., 1971. *Init. Repts. DSDP,* 8: Washington (U.S. Govt. Printing Office).

Walker, G.P.L., 1990. Geology and volcanology of the Hawaiian islands. *Pacific Sci.,* 44:315–347.

West, H.B., Garcia, M.O., Gerlach, D.C., and Romano, J., 1992. Geochemistry of tholeiites from Lanai, Hawaii. *Contrib. Mineral Petrol.,* 112:520–542.

Winterer, E.L., Riedel, W.R., et al., 1971. *Init. Repts. DSDP,* 7: Washington (U.S. Govt. Printing Office).

Wright, T.L., 1971. Chemistry of Kilauea and Mauna Loa lava in space and time. *Geol. Surv. Prof. Pap. U.S.,* Washington (U. S. Govt. Printing Office), 735:1–39.

* Abbreviations for names of organizations and publications in ODP reference lists follow the style given in *Chemical Abstracts Service Source Index* (published by American Chemical Society).

Date of initial receipt: 24 October 1992
Date of acceptance: 13 May 1993
Ms 136SR-204